PHOTONICS Research

Watt-level broadly wavelength tunable mode-locked solid-state laser in the 2 μm water absorption region

Wei Zhou,[1,2,4] Xiaodong Xu,[1,2] Rui Xu,[1,2] Xuliang Fan,[3] Yongguang Zhao,[1,2] Lei Li,[1,2] Dingyuan Tang,[1,2] and Deyuan Shen[1,2,*]

[1]Jiangsu Key Laboratory of Advanced Laser Materials and Devices, School of Physics and Electronic Engineering, Jiangsu Normal University, Xuzhou 221116, China
[2]Jiangsu Collaborative Innovation Center of Advanced Laser Technology and Emerging Industry, Jiangsu Normal University, Xuzhou 221116, China
[3]Department of Optical Science and Engineering, Fudan University, Shanghai 200433, China
[4]e-mail: weizhou@jsnu.edu.cn
*Corresponding author: shendy@fudan.edu.cn

Received 24 July 2017; revised 14 September 2017; accepted 14 September 2017; posted 15 September 2017 (Doc. ID 303157); published 17 October 2017

We report on broadly wavelength-tunable passive mode-locking with high power operating at the 2 μm water absorption band in a Tm:CYA crystal laser. With a simple quartz plate, stable mode-locking wavelengths can be tuned from 1874 to 1973 nm, with a tunable wavelength range up to ~100 nm and maximum output power up to 1.35 W. The bandwidth is narrow as ~6 GHz, corresponding to a high coherence. To our knowledge, this is the first demonstration of wavelength-tunable mode-locking with watt-level in the 2 μm water absorption band. The high temporal coherent laser can be further applied in spectroscopy, the efficient excitation of molecules, sensing, and quantum optics.

OCIS codes: (140.4050) Mode-locked lasers; (140.7090) Ultrafast lasers; (140.3580) Lasers, solid-state; (140.3070) Infrared and far-infrared lasers.

https://doi.org/10.1364/PRJ.5.000583

1. INTRODUCTION

Mode-locked Tm^{3+}, Ho^{3+}-doped lasers that emit with a wavelength around 2 μm are attracting increasing attention. The unique advantages such as high quantum efficiency, large emission bandwidth, "eye safe laser," and high temporal coherence make them promising candidates for applications in numerous cutting-edge research [1], next-generation optical communications [2], gas monitoring [3], and favorable pump sources of high-efficiency mid-infrared generation [4]. Based on the well-known atmospheric transparency windows around 2 μm (1.95–2.6 μm), ultrafast solid-state lasers with conventional Tm/Ho-doped crystals or ceramics, such as Tm:KYW crystal [5], Tm:Lu_2O_3 ceramic [6], Tm:LuAG crystal [7], Tm, Ho:$KY(WO_4)_2$ crystal [8], Ho:YAG ceramic [9], and Tm:LuAG ceramic [10] have been widely investigated. These laser oscillators deliver stable pulse trains with picosecond or subpicosecond durations, and the highest output average power is up to 1.21 W [7].

Particularly, water molecules demonstrate strong absorption from 1.8 to 1.95 μm, which matches well with the emission peaks of thulium ion near 2 μm [11,12]. This allow lasers operating at this region to demonstrate attractive potential in laser surgery [13], polymers processing [14], 3D laser printing [15], and attosecond pulses generation at the water window [16]. However, the strong absorption of water vapor [strongly absorbs more at ~1.94 μm (~114 cm^{-1}) than at ~1.5 μm (~10 cm^{-1}) and ~1 μm (~1 cm^{-1}) [12]] as well as the intrinsic multipeak and narrow emission spectrum of conventional gain medium make it difficult to obtain stable mode locking (ML) in the water absorption band [5,17]. Only a few works have reported mode-locked pulses with limited output power in this wavelength range [18,19]. Recently, the novel Tm:$CaYAlO_4$ (Tm:CYA) crystal with structure disorder and multisites has attracted increasing attention due to the large gain emission cross-section, high thermal conductivity, and the favorable broad emission band. This can support a broad wavelength-tuning range and a short pulse duration [20]. With this crystal, Kong *et al.* reported the first synchronous fundamental ML at 1960 nm [21]. Recently, Lan *et al.* reported a passively *Q*-switched Tm:CYA laser at 1929 nm, with output power of 490 mW and pulse duration 0.48 μs [22].

We have previously reported a first harmonic ML with Tm:CYA crystal [23]. In this paper, we report on a stable passive ML with broadly wavelength-tunable and high output power at 2 μm water absorption region for the first time, to the best of our knowledge. With a simple quartz plate, the mode-locked laser wavelengths can be tuned from 1874 to 1973 nm (~100 nm), with bandwidth as narrow as ~6 GHz, pulse repetition rate of 194 MHz, and maximum output average power up to 1.35 W. To the best of our knowledge, this is the highest output average power in 2 μm passive mode-locked bulk lasers and also the largest tunable bandwidth below 2 μm in Tm/Ho solid lasers.

2. EXPERIMENTAL SETUP

The laser is schematically shown in Fig. 1(a), which is similar in Ref. [23]. The Z-type laser cavity was constructed by four mirrors. The pump was a fiber-coupled laser diode with 105 μm core diameter and 0.22 numerical aperture (NA), at 790 nm. The pump beam was collimated and focused into the gain crystal with a diameter of ~100 μm. The a-cut Tm:CYA crystal with antireflectively coated from 1900 to 2100 nm was employed with a dimension of 3 mm × 3 mm × 6.1 mm, and a Tm^{3+} doping of 4 at.%. The laser beam diameter inside the gain crystal was 200 μm in sagittal and tangential planes, respectively. The SESAMs (BATOP GmBH) is designed to operate at 1800–2100 nm with a modulation depth of 1.2%, a relaxation time of 10 ps, and a saturation fluence of 70 $\mu J/cm^2$. The cavity mode diameter on the SESAMs was about 120 μm. The optical length is ~77 cm long, corresponding to the fundamental repetition rate of ~194 MHz. For optional wavelength tuning, a 1.74 mm thick quartz-crystal plate was inserted close to the SESAMs, acting as a spectrum filtering. The filter has a transmission of >99.6% from 1900 to 2100 nm. The optical axis of quartz filter is parallel to the plate surface.

An InAs photodetector with bandwidth of 12.5 GHz was employed to record pulse waveforms. An optical spectrum analyzer with a high resolution of 0.05 nm was used to monitor the spectrum. The radio frequency (RF) spectrum was measured by a 3 GHz spectrum analyzer. The pulse width was recorded by a commercial autocorrelator (Pulsecheck, APE).

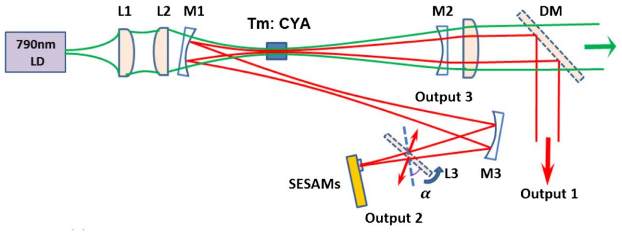

Fig. 1. Schematic of the Tm:CYA laser. L1 and L2 are the pump collimating and focusing lens (f = 100 mm), M1 and M2 are the highly reflective concave mirrors with the radius of curvature (ROC) of 100 mm, and the M2 is also the output coupler (OC) with output ratio of 10%, M3 is the highly reflective concave mirror, with the ROC of 200 mm, DM is the dichroic mirror (HR 2000 nm/AR 790 nm). L3 is a quartz-crystal-plate filter. α is the tilted angle, which equals the incidence angle of the ray between the plate surface and laser propagation direction. The effective output is the total of the three output ports (Output1, Output2, and Output3).

3. EXPERIMENTAL RESULTS AND DISCUSSION

Figure 2 shows the measured emission spectrum (at resolution of 0.05 nm) of the Tm:CYA crystal and the corresponding water absorption lines at room temperature of 25°C and relative air humidity of ~40% RH. The crystal has a spectrum bandwidth (FWHM) of nearly ~165 nm and shows many narrow multipeaks in the range from 1800 to 1950 nm, which matches well with the water vapor absorption lines calculated from the HITRAN database [24]. The irregular dips on the spectra (<1950 nm) are due to the absorption lines of the O-H bounds in atmosphere. The single-pass pump absorption ratio of 790 nm is measured to be 78%. At the continuous wave (CW) operation, the maximum output average power is up to 2 W at the incident pump power of 12 W with a slop efficiency of 17% and central wavelength of around 1950 nm. Because the longest wavelength of a pure electronic transition of Tm^{3+} ions in the CYA crystal is around 1.8 μm (see Fig. 2), the emission at longer wavelengths is owing to the vibronic nature of the laser transition, typical of Tm lasers [25]. With the SESAMs as the mode-locker, stable ML was obtained at the incident pump power of 4 W. At the pump power of 12 W, stable ML can still maintain with output average power up to 1.35 W and central wavelength of 1950 nm. But the mode-locked pulses split into two identical pulses with the same pulse-to-pulse duration, which is the so-called harmonic ML (HML) with pulse repetition rate exactly doubling of fundamental-order ML in Ref. [23].

Figure 3 shows the total and each port output power with wavelength tunable performance from mode-locked Tm:CYA lasers. After inserting the quartz plate and tuning the tilted angle α, stable ML can still be achieved. The corresponding central wavelength shifted with the tilted angle due to the birefringent filter of the quartz plate. With the 10% output coupler, the mode-locked wavelength can be achieved from 1874 to 1950 nm, with the output average power up to 1.15 W (at the maximum pump power of 12 W) at 1950 nm. When tuning the tilted angle, stable ML can maintain without adjusting the pump power or the cavity mirrors, indicating wavelength insensitive of the mode-locked pulses. This proves the high stability of the mode-locked laser, which is mainly due to the broad and relatively flat emission spectrum.

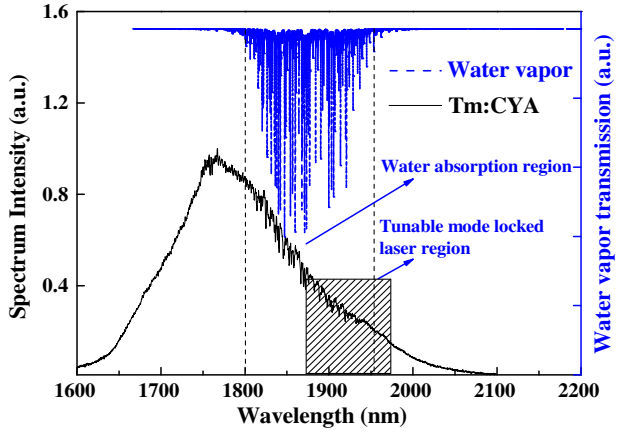

Fig. 2. Measured emission spectrums of Tm:CYA crystal and the calculated corresponding water absorption lines [24].

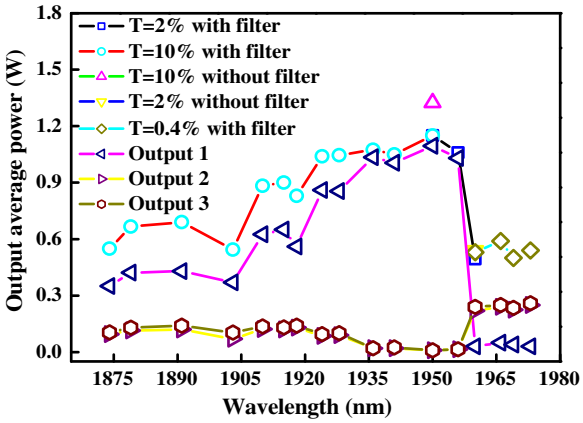

Fig. 3. Output power of tunable mode-locked Tm:CYA lasers with the quartz plate filter in the cavity at different OC mirrors of 10%, 2%, and 0.4%.

Although the emission peak with maximum intensity located at ~1770 nm, the output average power demonstrated a decreased tendency, which is due to the strong absorption of water vapor in this wavelength region [5]. With the lower output ratio of 2% and 0.4%, longer output wavelengths were obtained with the longest wavelength up to 1973 nm. This is the typical of quasi-three-level lasers such as Tm lasers and can be explained by taking into account the Boltzmann distribution of active ions in the upper and lower laser manifolds [26]. The power drop above 1950 nm is due to the low conversion efficiency caused by the low output ratio of ~2% and ~0.4%.

The mode-locked optical spectrums at different wavelengths are shown in Fig. 4. The spectrums have similar narrow bandwidth of ~0.1 nm and single master peak in the scale range of 100 nm. In the stable ML operation, a spectrum with double or multiple peak has not been observed, indicating the well optical filtering effect. Figure 4(b) shows the typical unstable Q-switching and stable ML operation at 1890 nm. The irregular ripples located on the peak in Q-switched ML (QSML) are

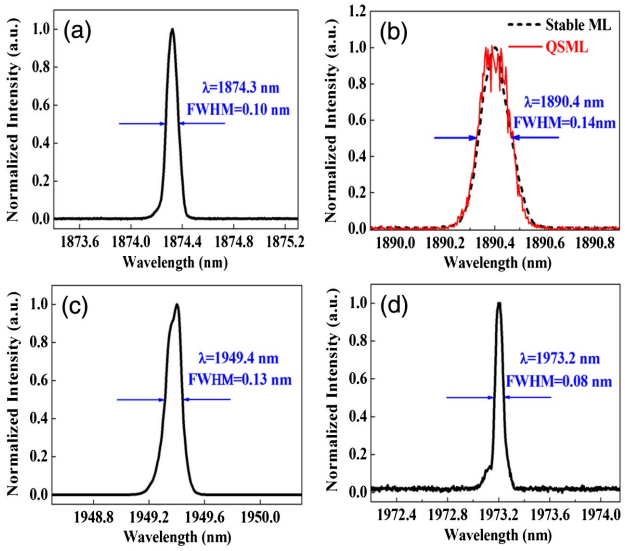

Fig. 4. Typical wavelength-tunable mode-locked optical spectrums at (a) 1874, (b) 1890, (c) 1949, and (d) 1973 nm.

caused by the longitudinal mode competition effect with the partially unlocked phase, which could degrade the stability of ML [27]. The narrowest bandwidth is 0.08 nm [Fig. 4(d)], corresponding to ~6.1 GHz. The obtained ML demonstrated smooth and single-peak spectra performances, without modulation ripples caused by the unstable Q-switching located on the spectrum peak. The smooth and single peak spectrum indicates the high stability of obtained ML without the interruption of Q-switching and the interruption flow of water vapor absorption in cavity. The spectrum also shows a Gauss shape.

Figure 5 demonstrates the temporal characteristics of mode-locked pulses at typical 1890 nm. The pulses amplitude stability is measured by the high-speed oscilloscope, with the amplitude intensity root mean square (RMS) noise of <0.3% [see Fig. 5(a)] and single pulse in a cavity [see Fig. 5(b)]. This confirms a high stability of pulse energy fluctuation. The repetition rate stability of the mode-locked laser, including the quartz plate filter, was characterized by the measurement of the RF spectrum, and the results are shown in Fig. 5(c), with negligible modulation components below −60 dB. At the resolution bandwidth (RBW) of 100 Hz, the typical RFs of mode-locked pulses at 1890 nm have a measured signal-to-noise (SNR) of 55 dB in Fig. 5(d). The corresponding frequency width of the noise component (FWNC) was measured to be 0.34 kHz. Following Ref. [28], the pulse-to-pulse energy fluctuations were estimated to be 1.9×10^{-3}. The relative timing jitter was estimated to be 4.5×10^{-4}. Considering the cavity period of ~5.1 ns, the frequency jitter is ~2.36 ps, which is low compared with the corresponding pulse duration. This indicates that the mode-locked laser in the water absorption region has high stability in temporal. The large emission bandwidth of the novel disorder Tm:CYA crystal and large pump intensity afforded the large gain, which balanced the loss caused by the water absorption, resulting in a stable wavelength-tunable ML in the water absorption region. Also the filtering effect of the quartz plate stabilized the wavelength and limited the generation of other wavelengths, which helps to stabilize ML operation.

For the temporal coherence, the autocorrelation traces of mode-locked pulses at 1890 and 1950 nm were measured, with results shown in Fig. 6. The relatively low SNR was due to the low response of the APE detector. Assuming the Gaussian-shaped hypothesis, the pulse duration was estimated to be ~46 ps and ~49 ps, respectively. The corresponding time-bandwidth product (TBP) was calculated to be 0.54 and 0.5, respectively. A slighter larger than the transformed value of 0.441. This indicates that the obtained pulses are slightly chirped, which is mainly caused by the uncompensated group velocity dispersion.

We also find that the mode-locked central wavelengths showed a blueshift tendency by increasing the tilted filter angle, which is shown in Fig. 7. At the 0° of tilted filter angle, the central wavelength stays the same at 1950 nm with the filter-free operation. The shortest wavelength of 1874 nm was achieved at the ~65°, while still keeping stable ML operation. Due to the relatively large aperture of Ø1″ and short cavity, available larger tunable tilted angle (>65°) was limited.

According to the wavelength-shift tendency noted above, ML with shorter wavelength (<1874 nm) could be further obtained by the well-controlled tilted angle of the quartz plate.

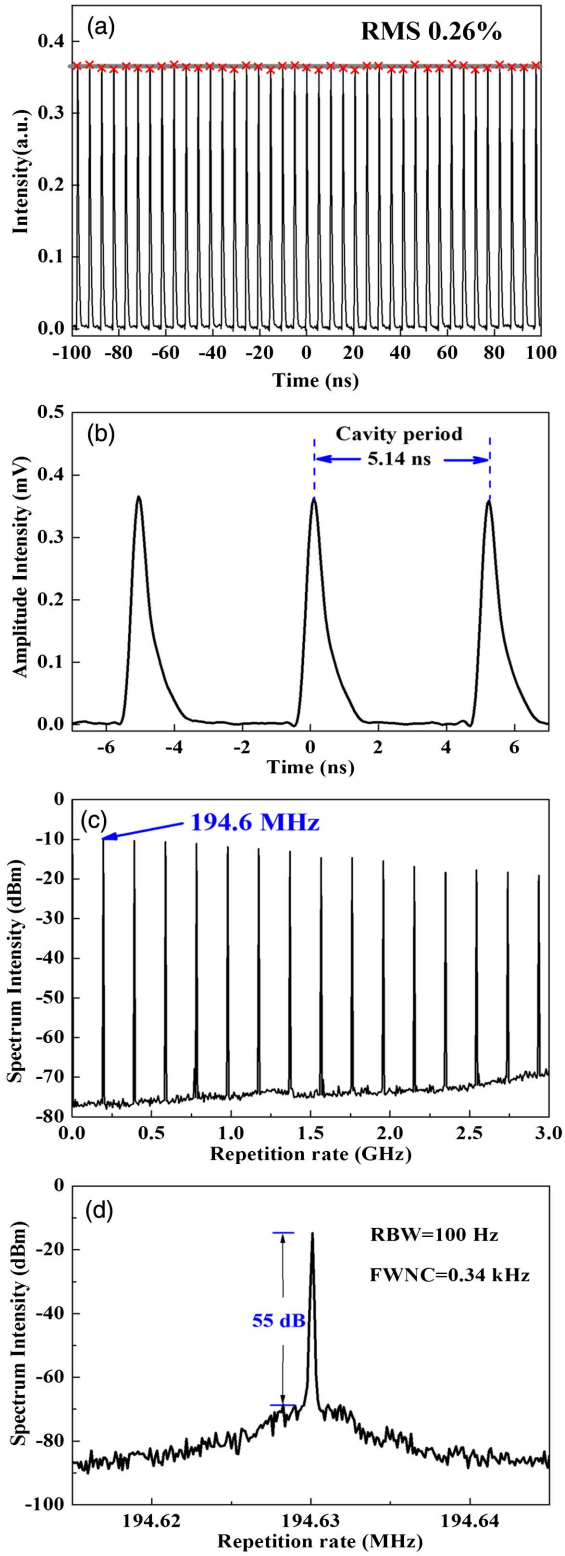

Fig. 5. Typical mode-locked pulses at 1890 nm. (a) Intensity trace of a real-time measurement showing 39 pulses with RMS noise below 0.3%; (b) measured single pulse; (c) RF spectrum with large span of 3 GHz; (d) RF spectrum with short span of 30 kHz.

The wavelength shifting demonstrated an approximately linear tendency with the tilted angle; this will enable easy control of wavelength selection by precisely rotating the quartz plate with a step motor.

For the wavelength-tunable mechanism, although the quartz plate (1.74 mm thick) played two roles in the wavelength tuning, the Birefringent filtering effect contributed more. For the Fabry–Perot (FP) resonant filtering effect, the free spectral range (FSR) is estimated to be 0.7 nm. This is much narrower than the obtained wavelength-tunable range of 76 nm, which can be neglected in the wavelength-tuning operation. However, for the

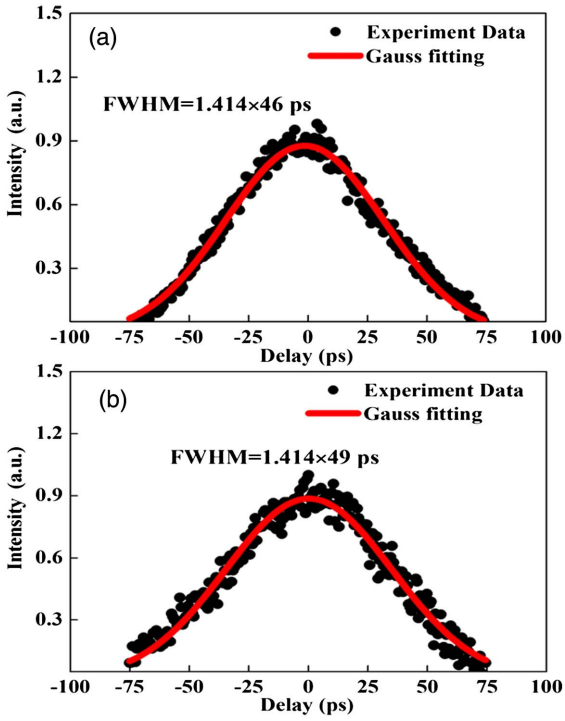

Fig. 6. Autocorrelation traces of ML at (a) typical 1890 and (b) 1950 nm.

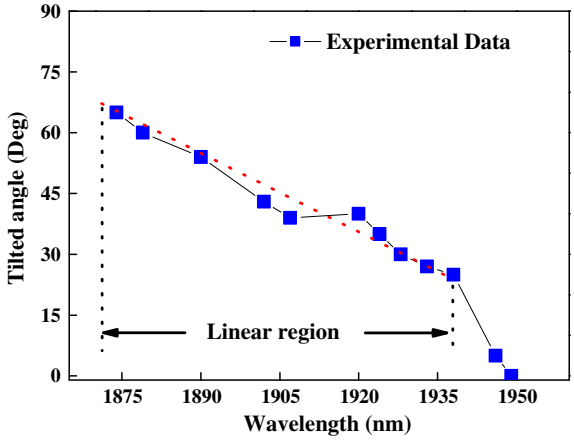

Fig. 7. Wavelength shift of ML with the tilted angle of the quartz plate at the typical 10% output ratio.

birefringent filtering effect, with the birefringence $\Delta n = 0.008$ of quartz crystal at 1.95 μm, the FSR is estimated to be ~268 nm [29]. This is much broader than the FSR of the FP resonant filtering, which can well support the obtained large wavelength-tunable range. Similar wavelength-tunable CW lasers were also obtained with the quartz plate [8,26].

The high output power and wide wavelength tunability are mainly attributed to the broad emission spectrum profile (>165 nm) of the novel disorder structure of Tm:CYA crystal. The high thermal conductivity and large emission cross-section of this crystal enable high-strength pumping and contributed to the high output. The long pulse duration of tens of picoseconds is caused by spectrum filtering of the multiple narrow peaks by the strong water molecule absorption, which can be clearly seen in Fig. 2; this is similar to the HML in our previous results [23]. Further exploration of the narrow bandwidth and long pulse duration is still needed.

4. CONCLUSION

In conclusion, we have demonstrated a watt-level wavelength-tunable mode-locked solid laser in 2 μm water absorption band for the first time, to our knowledge. Employing a simple quartz plate as an optical filter, the mode-locked wavelength can be tuned from 1874 to 1973 nm, resulting in a band-tunable-range of ~100 nm and narrow spectrum bandwidth of 6 GHz. At 1950 nm, the stable ML has an average output power up to 1.35 W and pulse duration of 49 ps, which is the highest output power in 2 μm passive mode-locked bulk oscillators. Due to the strong water absorption (main constituent of human tissue) around 1.9 μm, the obtained wavelength-tunable laser can be widely applied in diagnostic medical laser surgery, novel polymer processing, and gas sensing.

Funding. Natural Science Foundation of Jiangsu Province (BK20160221); Natural Science Foundation of Xuzhou, China (KC16SG247); Doctoral Research Funding of Jiangsu Normal University (15XLR024); Priority Academic Program Development of Jiangsu Higher Education Institutions (PAPD).

REFERENCES

1. K. Sugioka and Y. Cheng, "Ultrafast lasers—reliable tools for advanced materials processing," Light Sci. Appl. **3**, e149 (2014).
2. Z. Li, A. M. Heidt, N. Simakov, Y. Jung, J. M. O. Daniel, S. U. Alam, and D. J. Richardson, "Diode-pumped wideband thulium-doped fiber amplifiers for optical communications in the 1800–2050 nm window," Opt. Express **21**, 26450–26455 (2013).
3. E. De Tommasi, G. Casa, and L. Gianfrani, "High precision determinations of NH_3 concentration by means of diode laser spectrometry at 2.005 μm," Appl. Phys. B **85**, 257–263 (2006).
4. W. Q. Yang, B. Zhang, G. H. Xue, K. Yin, and J. Hou, "Thirteen watt all-fiber mid-infrared supercontinuum generation in a single mode ZBLAN fiber pumped by a 2 μm MOPA system," Opt. Lett. **39**, 1849–1852 (2014).
5. A. A. Lagatsky, S. Calvez, J. A. Gupta, V. E. Kisel, N. V. Kuleshov, C. T. A. Brown, M. D. Dawson, and W. Sibbett, "Broadly tunable femtosecond mode-locking in a Tm:KYW laser near 2 μm," Opt. Express **19**, 9995–10000 (2011).
6. A. A. Lagatsky, O. L. Antipov, and W. Sibbett, "Broadly tunable femtosecond Tm: Lu_2O_3 ceramic laser operating around 2070 nm," Opt. Express **20**, 19349–19354 (2012).
7. T. Feng, K. Yang, J. Zhao, S. Zhao, W. Qiao, T. Li, T. Dekorsy, J. He, L. Zheng, Q. Wang, X. Xu, L. Su, and J. Xu, "1.21 W passively mode-locked Tm:LuAG laser," Opt. Express **23**, 11815–11825 (2015).
8. A. A. Lagatsky, F. Fusari, S. Calvez, J. A. Gupta, V. E. Kisel, N. V. Kuleshov, C. T. A. Brown, M. D. Dawson, and W. Sibbett, "Passive mode locking of a Tm, Ho:$KY(WO_4)_2$ laser around 2 μm," Opt. Lett. **34**, 2587–2589 (2009).
9. Y. C. Wang, R. J. Lan, X. Mateso, J. Li, C. Hu, C. Y. Li, S. Suomalainen, A. HÄrkÖnen, M. Guina, V. Petrov, and W. Gribner, "Broadly tunable mode-locked Ho:YAG ceramic laser around 2.1 μm," Opt. Express **24**, 18003–18012 (2016).
10. C. Luan, K. Yand, J. Zhao, S. Zhao, T. Li, H. Zhang, J. He, L. Song, T. Dekorsy, M. Guina, and L. Zheng, "Diode-pumped mode-locked Tm:LuAG laser at 2 μm based on GaSb-SESAM," Opt. Lett. **42**, 839–842 (2017).
11. A. Godard, "Infrared (2-12 μm) solid-state laser sources: a review," C. R. Physique **8**, 1100–1128 (2007).
12. B. M. Walsh, "Review of Tm and Ho materials: spectroscopy and lasers," Laser Phys. **19**, 855–866 (2009).
13. F. M. P. Leclère, M. Schoofs, F. Auger, B. B. Ing, and S. R. Mordon, "Blood flow assessment with magnetic resonance imaging after 1.9 μm diode laser-assisted microvascular anastomosis," Lasers Surg. Med. **42**, 299–305 (2010).
14. M. Malinauskas, A. Žukauskas, S. Hasegawa, Y. Hayasaki, V. Mizeikis, R. Buividas, and S. Juodkazis, "Ultrafast laser processing of materials: from science to industry," Light Sci. Appl. **5**, e16133 (2016).
15. X. Y. Chen, Q. Gao, X. L. Wang, and X. D. Li, "Experimental design and parameter optimization for laser three-dimensional (3-D) printing," Laser Eng. **33**, 189–196 (2016).
16. M. C. Chen, P. Arpin, T. Popmintchev, M. Gerrity, B. Zhang, M. Seaberg, D. Popmintchev, M. M. Murnane, and H. C. Kapteyn, "Bright, coherent, ultrafast soft x-ray harmonics spanning the water window from a tabletop light source," Phys. Rev. Lett. **105**, 173901 (2010).
17. F. Wu, W. C. Yao, H. T. Xia, Q. Y. Liu, M. M. Ding, Y. G. Zhao, W. Zhou, X. D. Xu, and D. Y. Shen, "Highly efficient continuous-wave and Q-switched Tm:$CaGdAlO_4$ laser at 2 μm," Opt. Mater. Express **7**, 1290–1294 (2017).
18. W. B. Cho, A. Schmidt, J. H. Yim, S. Y. Choi, S. Lee, F. Rotermund, U. Griebner, G. Steinmeyer, V. Petrov, X. Mateos, M. C. Pujol, J. J. Carvajal, M. Aguiló, and F. Díaz, "Passive mode-locking of a Tm-doped bulk laser near 2 μm using a carbon nanotube saturable absorber," Opt. Express **17**, 11007–11012 (2009).
19. N. Coluccelli, G. Galzerano, D. Gatti, A. Di Lieto, M. Tonelli, and P. Laporta, "Passive mode-locking of a diode-pumped Tm:$GdLiF_4$ laser," Appl. Phys. B **101**, 75–78 (2010).
20. S. F. Gao, Z. Y. You, J. L. Xu, Y. J. Sun, and C. Y. Tu, "Continuous wave laser operation of Tm and Ho co-doped $CaYAlO_4$ and $CaGdAlO_4$ crystals," Mater. Lett. **141**, 59–62 (2015).
21. L. C. Kong, Z. P. Qin, G. Q. Xie, X. D. Xu, J. Xu, P. Yuan, and L. J. Qian, "Dual-wavelength synchronous operation of a mode-locked 2-μm Tm:$CaYAlO_4$ laser," Opt. Lett. **40**, 356–358 (2015).
22. J. L. Lan, X. Y. Zhang, Z. Y. Zhou, B. Xu, H. Y. Xu, Z. P. Cai, N. Chen, J. Wang, X. D. Xu, R. Soulard, and R. Moncorgé, "Passively Q-switched Tm:$CaYAlO_4$ laser using a MoS_2 saturable absorber," IEEE Photon. Technol. Lett. **29**, 515–518 (2017).
23. W. Zhou, X. L. Fan, H. Xue, R. Xu, Y. G. Zhao, X. D. Xu, D. Y. Tang, and D. Y. Shen, "Stable passively harmonic mode-locking dissipative pulses in 2 μm solid-state laser," Opt. Express **25**, 1815–1823 (2017).
24. http://hitran.iao.ru/molecule.
25. N. Coluccelli, G. Galzerano, F. Cornacchia, A. Di Lieto, M. Tonelli, and P. Laporta, "High-efficiency diode-pumped Tm: $GdLiF_4$ laser at 1.9 μm," Opt. Lett. **34**, 3559–3561 (2009).
26. R. C. Stoneman and L. Esterowitz, "Efficient, broadly tunable, laser-pumped Tm:YAG and Tm:YSGG cw lasers," Opt. Lett. **15**, 486–488 (1990).
27. L. A. Zenteno, H. Po, and N. M. Cho, "All-solid-state passively Q-switched mode-locked Nd-doped fiber laser," Opt. Lett. **15**, 115–117 (1990).
28. D. von der Linde, "Characterization of the noise in continuously operating mode-locked lasers," Appl. Phys. B **39**, 201–217 (1986).
29. Y. B. Liao, *Polarization Optics* (Science Publishing, 2003).